Molecular Spin-Flip Loss and a Dual Quadrupole Trap

David Reens,* Hao Wu,* Tim Langen,† and Jun Ye
JILA, National Institute of Standards and Technology and the University of Colorado and Department of Physics, University of Colorado, Boulder, Colorado 80309-0440, USA
(Dated: September 12, 2017)

Doubly dipolar molecules exhibit complex internal spin-dynamics when electric and magnetic fields are both applied. Near magnetic trap minima, these spin-dynamics lead to enhancements in Majorana spin-flip transitions by many orders of magnitude relative to atoms, and are thus an important obstacle for progress in molecule trapping and cooling. We conclusively demonstrate and address this with OH molecules in a trap geometry where spin-flip losses can be tuned from over 200 s^{-1} to below our 2 s^{-1} vacuum limited loss rate with only a simple external bias coil and with minimal impact on trap depth and gradient.

The ultracold regime extends toward molecules on many fronts [1]. Since the earlier condensation of short-lived homonuclear alkali dimers near Feshbach resonances [2–4], KRb polar molecules have reached lattice quantum degeneracy [5] and other heterogeneous bialkalis continue to progress [6–10]. Recently developed laser cooling strategies are tackling certain nearly vibrationally diagonal molecules [11–16]. A diverse array of alternative strategies have succeeded to greater or lesser extents on other molecules [17–23]. All of these molecules will require secondary strategies like evaporation or sympathetic cooling to make further gains in phase space density [24–26]. They also may face a familiar challenge: spin flip loss near the zero of a magnetic trap, but dramatically enhanced for many doubly dipolar molecules due to their internal spin dynamics in mixed electric and magnetic fields.

The knowledge of spin flips or Majorana hops as an eventual trap lifetime limit predates the very first magnetic trapping of neutrals [27]. Spin flips were directly observed near 50 μK and overcome with a time-orbiting potential trap [28] and a plugged dipole trap [29], famously enabling the first production of Bose-Einstein condensates. Motivated by the interest in dipolar molecules in mixed fields for quantum chemistry, precision measurement and many-body physics, we previously investigated loss of magnetically trapped hydroxyl radicals (OH) with applied electric field [30]. This trap loss occurred for substates of OH's $X^2\Pi_{J=3/2}$ ground state manifold other than the most well trapped one (positive parity and full spin polarization, $|f, m_J = 3/2\rangle$, blue in Fig. 1). Due to the closely spaced parity doublet, a general feature of Hund's case (a), these states intersect opposite parity states at non-zero magnetic fields, where electric fields can then open avoided crossings and cause trap loss. We now identify internal spin-dynamics leading to trap loss near zero magnetic field even for the most well trapped state and as warm as 50 mK.

These internal spin-dynamics are subtle, having eluded two previous investigations of note: In [31] the analogues of atomic spin-flip loss for molecules in mixed fields were modeled, and a magnetic quadrupole trap for OH molecules with superposed electric field was specifically addressed. It was concluded that no significant loss enhancement due to electric field would be evident. This is true only for the approximate $^2\Pi_{1/2}$ Hamiltonian used in that study. In [32] it was correctly noted that Hund's case (a) molecules maintain a quantization axis in mixed fields. The states of the molecule were shown to align with one of the two quantization axes given by the vec-

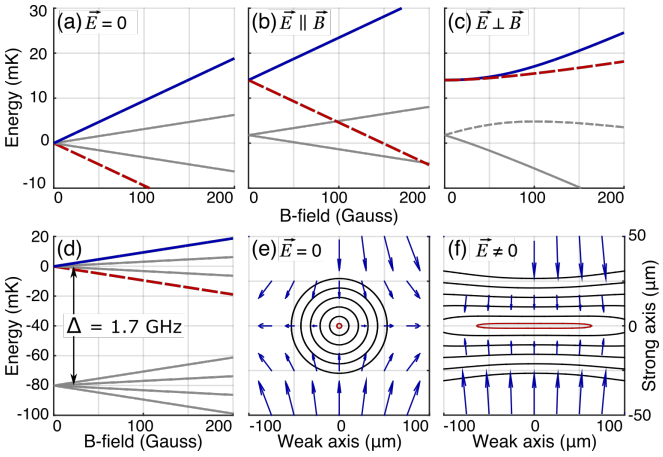

FIG. 1. A uniform electric field, added to magnetically trapped molecules for dipolar studies or other purposes, can lead to spin-flip losses. Four Zeeman split lines in OH's $X^2\Pi_{3/2}$ manifold are shown (a-c), with the trapped $|f, 3/2\rangle$ state in blue and its spin-flip partner $|f, -3/2\rangle$ in dashed red. These states are shown with no electric field (a), with $|\vec{E}| = 150$ V/cm and $\vec{E} \parallel \vec{B}$ (b), and with $\vec{E} \perp \vec{B}$ (c). Note the vastly reduced red-blue splitting in the latter case. The gray close dashes (c) denote the $|f, 1/2\rangle$ state, which is briefly discussed in the main text. The opposite parity ($|e\rangle$) manifold is split by Δ (d). Energy splitting contours are shown every 40 MHz near the zero of a 2 T/cm magnetic quadrupole trap for OH molecules [30] with $\vec{E} = 0$ (e), and with uniform $E = 150$ V/cm along the strong axis of the quadrupole (f). The vectors are $\mu_{\text{eff}}\vec{B} \pm d_{\text{eff}}\vec{E}$, where the sign is positive above the horizontal centerline and negative below, which represents the proper quantization axis for magnetically trapped molecules. Note the drastic widening of the lowest contour (red), the culprit for molecular spin-flip loss enhancement.

tors $d_{\rm eff}\vec{E} \pm \mu_{\rm eff}\vec{B}$ [33], $\mu_{\rm eff}$ and $d_{\rm eff}$ the effective dipole moments of the molecule in uncombined fields. It was asserted that this would maintain quantization near the zero of a quadrupole trap and avoid spin-flip loss, but as we now describe, the loss is actually enhanced.

We begin with an intuitive explanation of the loss enhancement based on molecular orientation. Consider a magnetic quadrupole trap, where a weak-field seeking molecule remains trapped insofar as it adiabatically follows the field direction. This is only challenging near the trap center where the magnetic field is vanishingly small, causing spin-flips. When electric field is added, it dominates in the trap center. Now suppose a molecule initially follows the quantization axis $d_{\rm eff}\vec{E} + \mu_{\rm eff}\vec{B}$ and is in the hemisphere where $\phi = \vec{E}\cdot\vec{B} > 0$, i.e. the fields are closer to parallel than antiparallel. During its orbit, $\vec{B}$ continuously rotates while $\vec{E}$ maintains its lab frame orientation, so that eventually $\phi < 0$ and $\vec{E}$ and $\vec{B}$ are closer to anti-parallel. Now the length of the quantization axis $d_{\rm eff}\vec{E} + \mu_{\rm eff}\vec{B}$, which is proportional to the field induced energy shift of the molecule, actually decreases with increasing $|B|$. The molecule is then magnetically strong field seeking and is lost. Therefore, to remain well-trapped a molecule must have the quantization axis $d_{\rm eff}\vec{E} + {\rm sign}(\phi)\mu_{\rm eff}\vec{B}$, so that an increase in magnitude of the magnetic field increases its potential energy. Whenever ϕ changes sign, even far from the trap center, there will be a chance of spin-flip associated with the molecule's propensity to maintain its quantization axis rather than remain in the well-trapped state. Since ϕ is a continuous scalar defined in 3D, $\phi = 0$ is a contour level of ϕ and thus always corresponds to a 2D surface defined by $\vec{E} \perp \vec{B}$; in the case of a magnetic quadrupole with homogeneous E it is a plane. This contrasts with atomic spin-flip loss, which does not favor a particular plane but occurs in a small ellipsoidal region near to the trap center.

This intuition agrees with a more rigorous analysis of the energy splitting G between the trapped state and its spin-flip partner. By diagonalizing the approximate eight state ground molecular Hamiltonian for OH, subtracting the relevant state energies and Taylor expanding, we find:

$$G(\mathcal{B}_\perp, \mathcal{B}_{||}, \mathcal{E}) = \mathcal{B}_{||} + \mathcal{B}_\perp^3 \frac{\Delta^2}{\mathcal{E}^4} + \mathcal{O}(\mathcal{B}_{||}^2, \mathcal{B}_\perp^4) \qquad (1)$$

Here $\mathcal{B} = \mu_{\rm eff}\vec{B}$ and $\mathcal{E} = d_{\rm eff}\vec{E}$, the magnetic field is considered in parallel ($\mathcal{B}_{||}$) and perpendicular ($\mathcal{B}_\perp$) components relative to the electric field, Δ is the lambda doubling, and G is the energy gap between the trapped state and its spin-flip partner. The relevant splitting between spin flip partner states reaches a deep minimum whenever $B_{||} = 0$, where the remaining Zeeman splitting is reduced from linear to cubic in magnetic field (Fig. 1a-c). This reduction in the Zeeman splitting from linear to cubic is in fact a well known phenomenon in the precision measurement community [34, 35], and experimentalists have exploited it for the suppression of unwanted influence from magnetic fields in measurements of the electron electric dipole moment. However, in the case of applying mixed fields during trapping, this suppression is not beneficial but rather detrimental, and the reduced splitting creates a broad plane in which spin-flips can occur (Fig. 1e-f).

TABLE I. Enhancements (η) and loss rates (Γ) for OH with typical applied fields. Zero field values are equivalent to atomic spin-flip loss. Electric field is required during evaporation and spectroscopy to open avoided crossings for $|e\rangle$ parity states [25, 30], or applied for polarization of the molecules to study collisions [36]. Background loss is 2 s^{-1}, experiment length 100 ms.

E (V/cm)	55 mK		5 mK		Purpose
	η	$\Gamma\,(s^{-1})$	η	$\Gamma\,(s^{-1})$	
0	1	0.02	1	1.3	Zero Field
300	5	0.1	9	11	Evaporation
550	17	0.3	40	50	Spectroscopy
3000	1000	19	1600	2000	Polarizing

To deduce the effect of this loss plane on the ensemble, we consider molecular trajectories in light of the Landau Zener formula:

$$P_{\rm hop} = e^{-\delta^2/\hbar v_z dG/dz}, \qquad (2)$$

which relates the probability of diabatically hopping between two states $P_{\rm hop}$ to the energetic coupling between the states δ and the rate of approach of the energy levels $\dot{G} = v_z dG/dz$. Here z and v_z are normal to the plane, and we neglect the component of $\dot{G}$ due to the other coordinates since from Eqn. 1 it is clear that dG/dz dominates. We can also set δ to the minimum energy gap along the trajectory, which is found in the plane. This facilitates direct numerical computation of loss rates by integrating the molecule flux through the plane for a thermal distribution, weighted by the hopping probability. We perform these integrations for OH in our previous 2 T/cm magnetic quadrupole [37] under various electric fields of interest (Tab. I).

It is also possible to proceed algebraically, which is useful for understanding the scaling of the effect with various parameters. This yields a loss electric field induced loss enhancement factor of

$$\eta = \left(\frac{d_{\rm eff}E}{\sqrt{\kappa\Delta}}\right)^{8/3}. \qquad (3)$$

Here κ is a characteristic energy scale for spin-flips that can be derived by setting $P = 1/e$ in Eqn. 2 and solving for δ. To get η, one simply compares the areas of the κ valued energy contours with and without electric field, solving $G(0, \mathcal{B}_{||}, \mathcal{E}) = \kappa$ from Eqn. eqn:energetics in the former case. It is interesting to note that in the limit of small Δ or linear Stark effect, the loss enhancement increases without bound. This makes sense from Eqn. 1, where we see that without Δ, $G = 0$ in the entire $\vec{E} \perp \vec{B}$ plane.

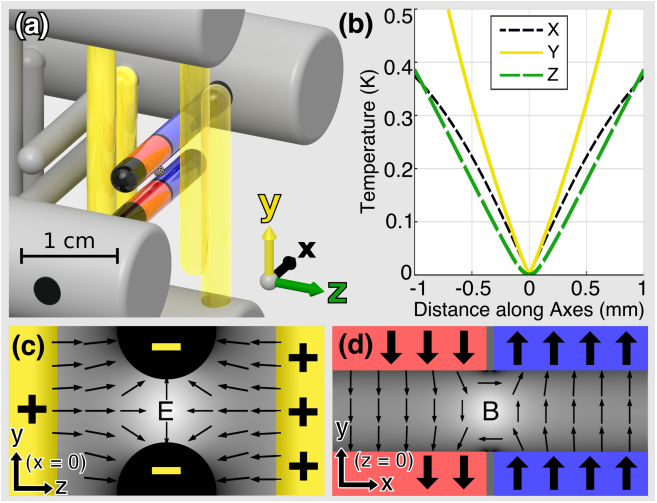

FIG. 2. The last six pins of our Stark decelerator [37] form the trap (a), which is 0.45 K deep with trap frequency $\nu \approx 4$ kHz (b). Along y the trap is bounded by the 2 mm pin spacing. The yellow pins are positively charged and the central pin pair negatively, which forms a 2D electric quadrupole trap with zero along the x-axis. This is shown for the $x=0$ plane (c), with yellow pins artificially projected for clarity since they don't actually intersect the plane. The central pins are magnetized, with two domains each. Blue indicates magnetization along $+\hat{y}$, red along $-\hat{y}$. These domains produce a magnetic quadrupole trap with zero along the z-axis, shown in the $z=0$ plane (d).

Returning to the numerical approach, we note that the direct integration of flux is a key improvement relative to our previous work [36], where electric fields were applied in our magnetic quadrupole trap to study their effect on collisions. The mechanism of molecular spin-flip loss was correctly identified in [36], and an appendix of that work describes the effect well. However, no separate experimental demonstration could be performed to verify or ascertain its magnitude since the application of electric field enhances trap loss both by spin-flips and inelastic collisions. A numerical deconvolution attempt was made based on the expected single versus two-body influence of the two effects, but the direct integration of flux was not performed, resulting in a three-fold underestimate of the loss magnitude. This ends up explaining a significant portion of the effect previously attributed to collisions, and is discussed further in [38]. In light of this significant influence of the spin-flip loss effect, it becomes especially important to perform direct experimental verification. We now present a new trap where the enhanced molecular spin-flip loss can be conclusively experimentally demonstrated without any convolved collisional effects, and where our loss-flux calculations can be clearly tested.

Our idea is to use a pair of 2D quadrupole traps, one magnetic and the other electric, with orthogonal centerlines (Fig. 2):

$$\vec{B} = B'x\hat{y} - B'y\hat{x} \qquad \vec{E} = E'y\hat{y} - E'z\hat{z} \tag{4}$$

We achieve these fields in a geometry that matches our Stark decelerator [19]. This geometry has $\vec{E} \perp \vec{B}$ in both the $x=0$ and $y=0$ planes, and $\mu_{\text{eff}}B < d_{\text{eff}}E$ in a large cylinder surrounding the z-axis- a perfect recipe for large spin-flip losses. However, by adding a small magnetic field $\vec{B} = B_{\text{coil}}\hat{z}$ along the centerline of the magnetic quadrupole with an external bias coil, a dramatic change can be made to the surfaces where $\vec{E} \perp \vec{B}$ with only a tiny change to the trapping potential.

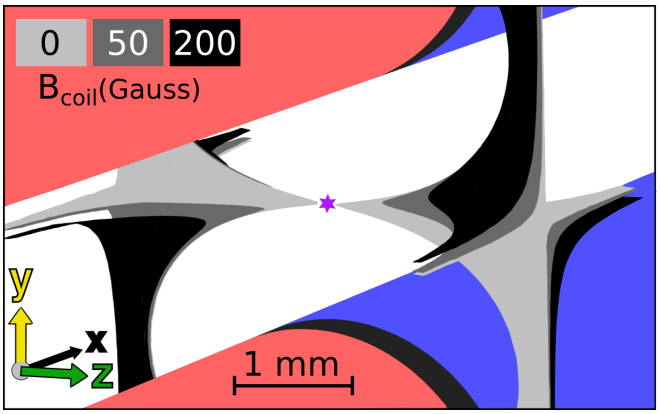

FIG. 3. Surfaces where spin-flips can occur ($\vec{E} \perp \vec{B}$, $\mu_{\text{eff}}B < d_{\text{eff}}E$) are shown for three values of B_{coil} in light gray, dark gray, and black. The magnetic pins are shown as in Fig. 2 for context. The purple star marks the trap center, to which molecules are confined within a ~1 mm diameter.

B_{coil} morphs the $\vec{E} \perp \vec{B}$ surface from a pair of planes into a hyperbolic sheet, pushing it away from the z-axis where the magnetic field is smallest. Algebraically, $\vec{E} \perp \vec{B}$ occurs when $\vec{E} \cdot \vec{B} = B'E'xy - B_{\text{coil}}E'z = 0$ and hence $x \cdot y = z \cdot B_{\text{coil}}/B'$. In Fig. 3, the surfaces where $\vec{E} \perp \vec{B}$ for several B_{coil} magnitudes are calculated wherever the splitting there is small enough that a molecule of thermally average velocity orthogonal to the surface would have a $1/e$ or greater hopping probability. The loss regions ought to be tuned far enough from the trap center that molecules cannot access them. This is indeed what we observe, note the striking difference in trap lifetimes in Fig. 4a. With only 200 G bias field (the trap is 5 kG deep) the loss is suppressed below that due to background gas.

In order to further verify our calculations of loss by integration of molecule fluxes across $\vec{E} \perp \vec{B}$ surfaces, we perform these calculations for a diverse collection of loss surfaces obtained by translation of the magnetic pins in their mounts. This translation serves to disrupt the idealized 2D magnetic quadrupole by adding a small trapping field $\vec{B} \propto B'z\hat{z}$. This dramatically alters the $\vec{E} \perp \vec{B}$ surfaces, the magnitude of the fields on them, and the hopping probability across them. We perform this transla-

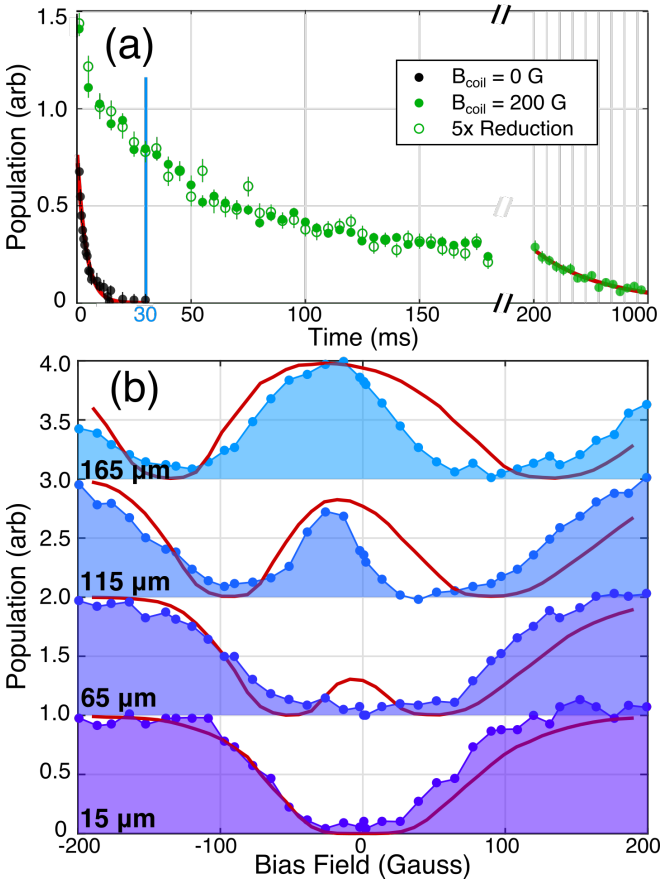

FIG. 4. Time traces (a) without bias field (black), with bias field (green dots), and with modulated density (green circles). One body fits (red) give loss rates of 200 s^{-1} without bias field and 2 s^{-1} with full bias field at long times, in agreement with our background gas pressure. At the fixed time 30 ms, population is shown as a function of both pin translation and bias field (b), for several values of pin translation, labeled relative to perfect alignment. Fits (red) are calculated by integrating the molecule flux of a thermal ensemble through surfaces where $\vec{E} \perp \vec{B}$.

tion in situ, and obtain a reasonable agreement (Fig. 4b). This is particularly noteworthy given that this direct integral calculation assumes a purely thermal distribution and doesn't involve the computation of any actual trajectories. The fits are performed using only temperature as a free parameter, which enters the calculation via the thermal distribution used for integration, and fits to 170 ± 20 mK. [39]. An intuitive explanation for the intriguing double well structure in population verses B_{coil} is that B_{coil} first translates the magnetic zero along the z-axis, overlapping it with larger electric fields at first before moving it out of the trap.

With strong experimental confirmation of the molecular spin-flip loss enhancement, we can move on to generalize beyond OH. Hund's case (a) states are most susceptible in the sense that smaller electric fields are sufficient to cause a significant problem, but with enough electric field any state exhibiting competition between electric and magnetic fields for alignment of the molecule or atom will be susceptible. One way to avoid competition is for the fields to couple to unrelated parts of the Hamiltonian, which happens to a limited extent for Hund's case (b) states without electron orbital angular momentum (Σ states, $\Lambda = 0$) [32]. In these states, which include most laser-cooled molecules thus far, the electric and magnetic fields couple to rotation and spin respectively, which are only related by the spin-rotation coupling constant γ. Since γ is usually in the tens of MHz [26], molecular spin-flip loss remains quite significant. The inclusion of hyperfine requires a careful case-by-case investigation. For OH, it would initially seem to add an extra splitting that could protect from spin-flips, but in fact the loss plane is only shifted slightly away from $\vec{E} \perp \vec{B}$ and retains the same area. For YO [40], certain hyperfine states can avoid spin-flip loss entirely when electric fields are applied. These states are characterized by significant electron-spin-to-nuclear-spin dipolar coupling, which results in a protective gap regardless of field orientation.

We can also generalize to other geometries with a simple loss suppression strategy: avoid $\mu_{\mathrm{eff}} B < d_{\mathrm{eff}} E$ where $\vec{E} \perp \vec{B}$. This is maximally violated by the magnetic quadrupole, where in a suitably small region even the smallest stray electric field dominates the magnetic. In a pure electrostatic trap, there is always some zero field parity splitting to prevent orientation-reversing spin flips. However, this same splitting pushes all states with the same sign of m_J very close to one another, leading to loss via Landau-Zener transitions other than the m_J to $-m_J$ spin-flip [41]. Intriguingly, the addition of a homogeneous magnetic field can actually suppress loss [42].

The present trap, in addition to providing the desired experimental testing ground for molecular spin-flip loss, produces large 5 T/cm trap gradients useful for maintaining high densities to facilitate collisional studies. This is in contrast with other strategies for plugging the hole of a magnetic trap which often lead to a reduction in trap gradient. With loss removed, we observe a population trend whose initially fast decay rate decreases over time (Fig. 4a, green dots), suggesting a two-body collisional effect. We test this by reducing the initial population fivefold but without changing its spatial or velocity distribution [38], and then scale the resulting trend by five (green circles). If collisions had contributed, this new trend would show less decay, but we observe no significant change. This seeming lack of collisions could be due to the warmer initial temperature of 170 mK, in contrast to the earlier work at and below 50 mK [25]. The results of this paper are important for the evaporation work, since the electric fields used for the RF knife ought to have caused a significant spin-flip loss effect, especially at low temperatures [38]. An alternative hypothesis for the population trend is the existence of chaotic trap orbits with long escape times [43]. Moving forward, we

aim to increase the density by means of several improvements [44, 45].

Molecule enhanced spin-flip loss arises in mixed electric and magnetic fields due to a competition between field quantization axes. We conclusively demonstrate and suppress this effect using our dual magnetic and electric quadrupole trap, which is also an ideal setting for further progress in collisional physics thanks to its large trap gradient. Our calculation of the magnitude of spin-flip loss via flux through surfaces where $\vec{E} \perp \vec{B}$ enables detailed predictions of how its location and magnitude ought to scale with bias field and trap alignment, which we experimentally verify. Our results correct existing predictions about molecular spin-flips in mixed fields and pave the way toward further improvements in molecule trapping and cooling.

We acknowledge the Gordon and Betty Moore Foundation, the ARO-MURI, JILA PFC, and NIST for their financial support. T.L. acknowledges support from the Alexander von Humboldt Foundation through a Feodor Lynen Fellowship. We thank J.L. Bohn, S.Y.T. van de Meerakker, and M.T. Hummon for helpful discussions. We thank Goulven Quéméner for his continued involvement in this research.

* Contributed equally. Email dave.reens@colorado.edu or hao.wu@colorado.edu.

† Present Address: 5. Physikalisches Institut and Center for Integrated Quantum Science and Technology (IQST), Universität Stuttgart, Pfaffenwaldring 57, 70569 Stuttgart, Germany

[1] L. D. Carr, D. DeMille, R. V. Krems, and J. Ye, New Journal of Physics **11**, 055049 (2009).

[2] M. Greiner, C. A. Regal, and D. S. Jin, Nature **426**, 537 (2003).

[3] M. W. Zwierlein, C. A. Stan, C. H. Schunck, S. M. F. Raupach, S. Gupta, Z. Hadzibabic, and W. Ketterle, Physical Review Letters **91**, 250401 (2003).

[4] S. Jochim, M. Bartenstein, A. Altmeyer, G. Hendl, S. Riedl, J. Hecker Denschlag, and R. Grimm, Science **302**, 2101 (2003).

[5] S. A. Moses, J. P. Covey, M. T. Miecnikowski, B. Yan, B. Gadway, J. Ye, and D. S. Jin, Science **350**, 659 (2015).

[6] T. Takekoshi, L. Reichsöllner, A. Schindewolf, J. M. Hutson, C. R. Le Sueur, O. Dulieu, F. Ferlaino, R. Grimm, and H.-C. Nägerl, Physical Review Letters **113**, 205301 (2014).

[7] J. W. Park, S. A. Will, and M. W. Zwierlein, Physical Review Letters **114**, 205302 (2015).

[8] M. Guo, B. Zhu, B. Lu, X. Ye, F. Wang, R. Vexiau, N. Bouloufa-Maafa, G. Quéméner, O. Dulieu, and D. Wang, Physical Review Letters **116**, 205303 (2016).

[9] L. R. Liu, J. T. Zhang, Y. Yu, N. R. Hutzler, Y. Liu, T. Rosenband, and K.-K. Ni, "Ultracold Molecular Assembly," (2017), arXiv:1701.03121.

[10] T. M. Rvachov, H. Son, A. T. Sommer, S. Ebadi, J. J. Park, M. W. Zwierlein, W. Ketterle, and A. O. Jamison, "Long-Lived Ultracold Molecules with Electric and Magnetic Dipole Moments," (2017), arXiv:1707.03925.

[11] B. K. Stuhl, B. C. Sawyer, D. Wang, and J. Ye, Physical Review Letters **101**, 243002 (2008).

[12] M. T. Hummon, M. Yeo, B. K. Stuhl, A. L. Collopy, Y. Xia, and J. Ye, Physical Review Letters **110**, 143001 (2013).

[13] J. F. Barry, D. J. McCarron, E. B. Norrgard, M. H. Steinecker, and D. DeMille, Nature **512**, 286 (2014).

[14] V. Zhelyazkova, A. Cournol, T. E. Wall, A. Matsushima, J. J. Hudson, E. A. Hinds, M. R. Tarbutt, and B. E. Sauer, Physical Review A **89**, 053416 (2014).

[15] B. Hemmerling, E. Chae, A. Ravi, L. Anderegg, G. K. Drayna, N. R. Hutzler, A. L. Collopy, J. Ye, W. Ketterle, and J. M. Doyle, Journal of Physics B: Atomic, Molecular and Optical Physics **49**, 174001 (2016).

[16] S. Truppe, H. J. Williams, M. Hambach, L. Caldwell, N. J. Fitch, E. A. Hinds, B. E. Sauer, and M. R. Tarbutt, Nature Physics (2017), 10.1038/nphys4241.

[17] J. M. Doyle, J. D. Weinstein, R. DeCarvalho, T. Guillet, and B. Friedrich, Nature **395**, 148 (1998).

[18] H. L. Bethlem, G. Berden, and G. Meijer, Physical Review Letters **83**, 1558 (1999).

[19] J. R. Bochinski, E. R. Hudson, H. J. Lewandowski, G. Meijer, and J. Ye, Physical Review Letters **91**, 243001 (2003).

[20] E. Narevicius, A. Libson, C. G. Parthey, I. Chavez, J. Narevicius, U. Even, and M. G. Raizen, Physical Review Letters **100**, 093003 (2008).

[21] A. Wiederkehr, H. Schmutz, M. Motsch, and F. Merkt, Molecular Physics **110**, 1807 (2012).

[22] A. Prehn, M. Ibrügger, R. Glöckner, G. Rempe, and M. Zeppenfeld, Physical Review Letters **116**, 063005 (2016).

[23] Y. Liu, M. Vashishta, P. Djuricanin, S. Zhou, W. Zhong, T. Mittertreiner, D. Carty, and T. Momose, Physical Review Letters **118**, 093201 (2017).

[24] L. P. Parazzoli, N. J. Fitch, P. S. Zuchowski, J. M. Hutson, and H. J. Lewandowski, Physical Review Letters **106**, 1 (2011).

[25] B. K. Stuhl, M. T. Hummon, M. Yeo, G. Quéméner, J. L. Bohn, and J. Ye, Nature **492**, 396 (2012).

[26] G. Quéméner and J. L. Bohn, Physical Review A - Atomic, Molecular, and Optical Physics **93**, 1 (2016).

[27] A. L. Migdall, J. V. Prodan, W. D. Phillips, T. H. Bergeman, and H. J. Metcalf, Physical Review Letters **54**, 2596 (1985).

[28] W. Petrich, M. H. Anderson, J. R. Ensher, and E. A. Cornell, Physical Review Letters **74**, 3352 (1995).

[29] K. B. Davis, M. O. Mewes, M. R. Andrews, N. J. van Druten, D. S. Durfee, D. M. Kurn, and W. Ketterle, Physical Review Letters **75**, 3969 (1995).

[30] B. K. Stuhl, M. Yeo, B. C. Sawyer, M. T. Hummon, and J. Ye, Physical Review A **85**, 033427 (2012).

[31] M. Lara, B. L. Lev, and J. L. Bohn, Physical Review A **78**, 033433 (2008).

[32] J. L. Bohn and G. Quéméner, Molecular Physics **111**, 1931 (2013).

[33] The authors use $\mu_{\text{eff}}\vec{B} \pm d_{\text{eff}}\vec{E}$. We reverse this to provide a more physical connection to our experiment, where the electric field is fixed.

[34] M. A. Player and P. G. H. Sandars, Journal of Physics B: Atomic and Molecular Physics **3**, 1620 (1970).

[35] J. J. Hudson, B. E. Sauer, M. R. Tarbutt, and E. A. Hinds, Physical Review Letters **89**, 023003 (2002).
[36] B. K. Stuhl, M. Yeo, M. T. Hummon, and J. Ye, Molecular Physics **111**, 1798 (2013).
[37] B. C. Sawyer, B. K. Stuhl, D. Wang, M. Yeo, and J. Ye, Physical Review Letters **101**, 203203 (2008).
[38] See Supplementary Materials.
[39] Calculation performed in COMSOL: Source Code.
[40] This is particularly relevant given the recently realized 3D MOT for YO.
[41] T. E. Wall, S. K. Tokunaga, E. a. Hinds, and M. R. Tarbutt, Physical Review A - Atomic, Molecular, and Optical Physics **81**, 1 (2010).
[42] S. A. Meek, G. Santambrogio, B. G. Sartakov, H. Conrad, and G. Meijer, Physical Review A - Atomic, Molecular, and Optical Physics **83** (2011), 10.1103/PhysRevA.83.033413.
[43] R. González-Férez, M. Iñarrea, J. P. Salas, and P. Schmelcher, Physical Review E **90**, 062919 (2014).
[44] U. Even, EPJ Techniques and Instrumentation **2**, 17 (2015).
[45] Y. Segev, N. Bibelnik, N. Akerman, Y. Shagam, A. Luski, M. Karpov, J. Narevicius, and E. Narevicius, Science Advances **3**, e1602258 (2017).